Desalination and Water Treatment
www.deswater.com

doi: 10.1080/19443994.2013.798840

52 (2014) 2450–2456
March

Taylor & Francis
Taylor & Francis Group

Water desalination using R141b gas hydrate formation

M. Karamoddin, F. Varaminian*

School of Chemical, Gas and Petroleum Engineering, Semnan University, Semnan, Iran
Tel./Fax: +98 231 3354280; email: fvaraminian@semnan.ac.ir

Received 28 September 2012; Accepted 28 March 2013

ABSTRACT

In this paper, water desalination was performed by R141b hydrate formation in systems containing refrigerant and a brine aqueous solution to determine of R141b hydrate growth rate and efficiency of process. Kinetic experiments were conducted with initial temperatures of 0, 2, and 4˚C with saline concentrations of 1, 2, 4, and 6% weight of NaCl and also with the molarity 0.304 mol/L of NaCl, KCl, $CaCl_2$, and $MgCl_2$ aqueous solutions. The results show that R141b hydrate formation rate depends on the saline concentration, initial temperature, and salt type. Moreover, the results of water desalination based on R141b hydrate formation indicate that the removal efficiency depends on the ionic size and electrical charge. Each dissolved mineral is removed in following order: $K^{+1}>Na^{+1}>Ca^{+2}>Mg^{+2}$ with 59–70% of efficiency.

Keywords: R141b; Gas hydrate; Growth rate; Desalination

---

1. Introduction

Clathrate hydrates are crystalline solid compounds. These crystals are composed of hydrogen-bonded water molecules (host molecules) and some other gas species (guest molecules). Water molecules form a cage-like structure at high pressure and low temperature conditions. The guest molecules, such as methane, ethane, and others hydrocarbons are trapped in the lattice and stabilize the structure [1,2].

During recent years, several techniques of desalination have been investigated by freezing and gas hydrate methods [3–6]. The hydration methods for desalination of seawater have been studied for the past 50 years considering the capability of gas hydrates to form a solid substance consisting of distilled water and hydrate former [7,8]. Gas hydrate formation as a novel method to produce potable water from seawater was proposed in 1940 and received significant attention in 1960s and 1970. In USA, many companies used this method in pilot plant scale [9]. Ngan and Englezos (1996) performed many experiments for the recovery of water from pulp mill effluents and 2.5% (wt) NaCl solutions through the hydrate formation of propane [10].

Also, refrigerant gas hydrates which are formed above 0˚C at moderate pressure can be considered as promising materials for energy storage and desalination of water, also, they are especially suitable for air conditioning systems [11,12]. The main problem in energy storage systems of gas hydrates is how to overcome the potential barrier at the interface between water phase and liquid (or gas) refrigerant to increase the rate of mass and heat transfer for refrigerants–water

---

*Corresponding author.

1944-3994/1944-3986 © 2013 Balaban Desalination Publications. All rights reserved.

systems for hydrate formation. Generally, refrigerants and water cannot be dissolved in each other and it usually takes a long time for the formation of gas hydrate [13,14].

In relation to refrigerants, a lot of researchers investigated different refrigerant hydrates. The phase equilibrium diagram of R22 refrigerant (CHF_2Cl) was measured at different concentrations of NaCl brine solution by Maeda et al. [15]. The influence of electrolytes (salts) which do not form hydrates was studied on the stability temperature of gas hydrates by Engelzos [16]. Also, Kubota et al. and Barduhn et al. applied this analysis for R152a and R21 hydrate formation, respectively [17,18]. Recently, the results of equilibrium temperature were presented for R141b hydrate formation in brine solution by Sandia National Laboratories [19].

In 2011, hydrate-based desalination was accomplished with novel apparatus design to extract dehydrated gas from a reactor containing hydrate slurries by Park et al. [3]. Moreover, different hydrate formers such as HFCs (refrigerants) have been suggested for further desalination research, since these substances are known to form hydrates under relatively mild conditions (lower pressure and higher temperature) which can decrease energy consumption during desalination process by hydrate [3].

In this study, HCFC141b refrigerant (CH_3CCl_2F) was chosen as hydrate former with structure II. R141b is suitable for engineering applications especially for the separation and desalination operation due to its lower saturation-pressure, low cost, and a low pressure (atmospheric) hydrate former that causes avoiding of working with high pressure process.

The nucleation and growth processes of R141b gas hydrate were studied by using pure water and saline solution in a cylindrical glass reactor. This study was investigated on the kinetics of R141b hydrate formation in the presence of sodium chloride inhibitor with different concentrations of NaCl aqueous solution and also in the presence KCl, $CaCl_2$, and $MgCl_2$ aqueous solutions with a similar molarity. Besides, the brine water desalination was performed by the separation of hydrate crystals from residual solution in different salts of NaCl, KCl, $MgCl_2$, and $CaCl_2$. The removal efficiency of dissolved salt in water was obtained by measuring the electrical conductivity of initial brine solution and final product (after separation of hydrate crystals). The parameters under investigation are the experimental temperature, the amount of dissolved salt in initial solution, the type of salt, the purity of the produced water phase with respect to salt, and the rate of the hydrate formation.

2. Experimental process

2.1. Materials

NaCl, KCl, $CaCl_2$, and $MgCl_2$ with 99.5% purity and R141b liquid with 99.5% purity were purchased from Merck and Isceon companies, respectively. De-ionized water was used in all the experiments.

2.2. Apparatus

Experiments were performed in a setup consisting of a reactor, a jacket for heat transfer, and a data acquisition system. This apparatus is shown in Fig. 1.

Hydrate formation was conducted in a magnetic stirrer batch reactor that was capable of ambient pressure. The reactor was composed of a cylindrical pyrex glass tube with height of 12 cm and diameter of 6 cm. The volume of the reactor was 500 cc. A jacket was used for the heating and cooling of system and the reactor temperature was controlled by ethylene glycol flowing through an external circulating temperature bath in the jacket. The electrical conductivity of the solution was measured using a conductivity meter (AQUALYTIC/AL20CON) with accuracy 0.1 μS/cm. The temperature was measured by PT100 thermometers (±0.1 K). Temperature measurements were acquired through a data acquisition system driven by a personal computer. Mixing is an important parameter in the experimental measurements because the hydrate formation experiments are necessarily conducted in

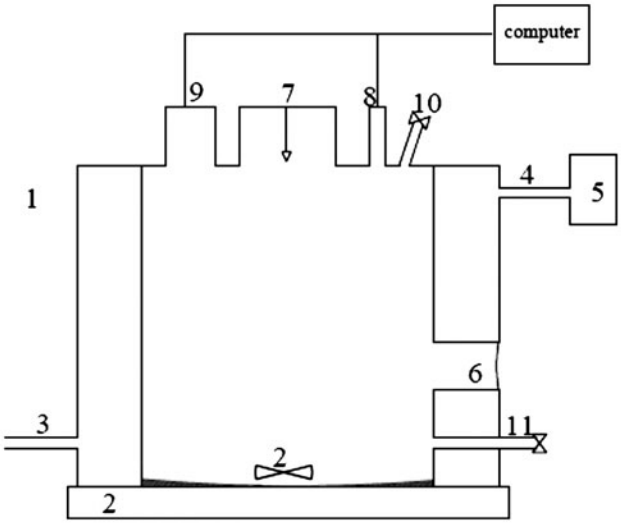

Fig. 1. Experimental setup: hydrate formation apparatus, (1) reactor, (2) magnet stirrer, (3, 4) heat jacket, (5) cooling unit, (6) view window, (7) input site, (8) thermometer sensor, (9) conductivity meter sensor, (10) gas valve, and (11) drain valve.

multiphase systems consisting of one or two liquid phases, a solid hydrate phase, and a gas phase. In this study, the experimental cell was placed in a magnetic stirrer (Heidolpg-Hei-mixs) with a stirring speed controller for mixing. All experiments were operated by using the stirrer with similar speed.

2.3. Experimental procedure: hydrate formation

R141b refrigerant forms the hydrate of structure II under atmospheric pressure at a temperature lower than 8.4˚C. The equation of the hydration reaction is [12,13]:

$$R + 17H_2O \rightarrow R17H_2O + \Delta H \quad (1)$$

According to Eq. (1), the weight ratio of water to R141b is 2.617. Also, ΔH in Eq. (1) is the heat of formation. The value of heat formation was presented experimentally to be about 334 kJ/kg [12]. The thermodynamic stability of R141b hydrate was investigated by several groups [12,13,19].

The normal boiling point of R141b refrigerant is about 38˚C, so, R141b was in the liquid state in the experiments described. The amount of initial solution injected into the reactor was 300 cc for each experiment. Considering that the weight ratio of water to R141b is 2.617, the aqueous solution (pure water or salt solution) and R141b liquid were 225 and 75 cc, respectively. The prerequisite amount of determined salts was weighed on an electronic balance (±0.01 gm) and dissolved in 225 cc of de-ionized water. Then, brine solution and R141b liquid were mixed together and poured into the reactor. The magnetic stirrer was turned on at a specified speed. The temperature of cooling unit must be fixed on appropriate value until the temperature of solution in the reactor reaches to the operation temperature (initial temperature: 0, 2, and 4˚C). After achieving stability, the temperature of the solution was logged using data acquisition system. The temperature rises during hydrate formation because of heat generation until the equilibrium temperature of R141b hydrate is acheived.

The hydration characteristics of a static reactor and growth morphology were described through the photos taken during the growth and decomposition processes by Xie et al. Also, they presented the temperature trends of the process [20].

After the completion of hydrate formation and restability, the separation of hydrate crystals from residual solution was performed by squeezing operation. Therefore, the adequate amount of crystal (hydrate slurry) was extracted from the head of reactor by a spatula and R141b hydrate slurries were supplied to a syringe as cylinder–piston. The end part of the syringe had passing holes with similar sizes. By pressing this syringe, the residual waters separated from hydrate crystal and flew out through the small passing holes in the end of the syringe. Then, the hydrate was compressed as pellet and was issued from the syringe easily. After pelletizing, hydrate pellets must be heated until the hydrate former vaporizes because of the low boiling point of R141b. In this study, the effect of salt type was investigated on the separation process too.

3. Results and discussion

3.1. Characteristics of gas hydrate growth

To investigate the kinetic behavior associated with R141b hydrate in desalination process, experiments were performed at initial temperatures of 0, 2, and 4˚C for saline concentrations of 1, 2, 4, and 6% weight of NaCl and also with 0.304 mol/L molarity of NaCl, KCl, $CaCl_2$, and $MgCl_2$ aqueous solutions at similar condition of mixing. The experiments were performed three times for obtaining reliable and confirmable data. Also, the error bar was about ±0.2˚C in measurement of temperature.

The R141b gas hydrate formation process contains three periods [19,20]: (1) The cooling stage: the period during which the brine solution and R141b are cooled and the temperatures decrease to the setting temperature before the formation of R141b hydrate. (2) The nucleation stage: the part during which the temperature of solution changes very slowly (temperature stability on T_{in}) and the crystal nuclei appear. The required time for the nucleation process is called the induction time. (3) The growth stage: the period of hydrate formation where the temperature suddenly increases to reach equilibrium temperature of R141b hydrate (T_{eq}) [19,20]. When the temperature falls again, the crystal growth stops [20].

Fig. 2 shows the temperature–time profile of the R141b hydrate experiment at an initial temperature of 0˚C for different concentrations of NaCl saline solution. As seen in Fig. 2, the rate of temperature growth (proportionate to formation rate) decreases by increasing saline concentration, and the induction and formation time for R141b hydrate process rise due to salt inhibition potential.

Figs. 3 and 4 show the temperature–time profile of hydrate experiment at different initial temperatures for pure water and 4% saline solution, respectively. The range of temperature variations is not very sizable during R141b hydrate formation process. So the experiments of hydrate formation were accomplished only for 0 and 4% saline solution where the

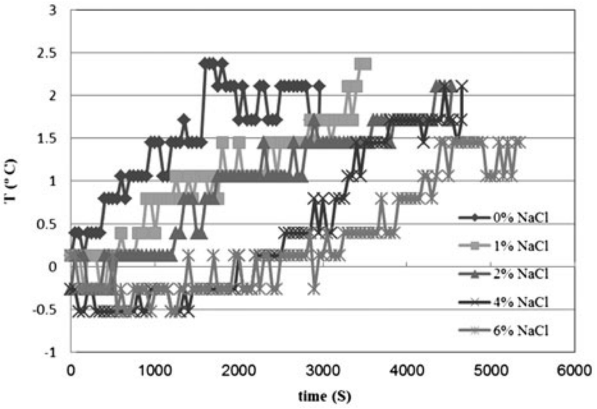

Fig. 2. Temperature–time profile during R141b hydrate formation at initial temperature of 0°C for different concentrations of NaCl.

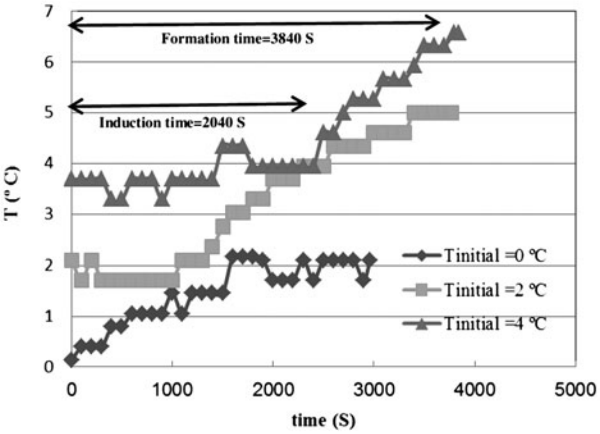

Fig. 3. Temperature–time profile during R141b hydrate formation at different initial temperatures for pure water.

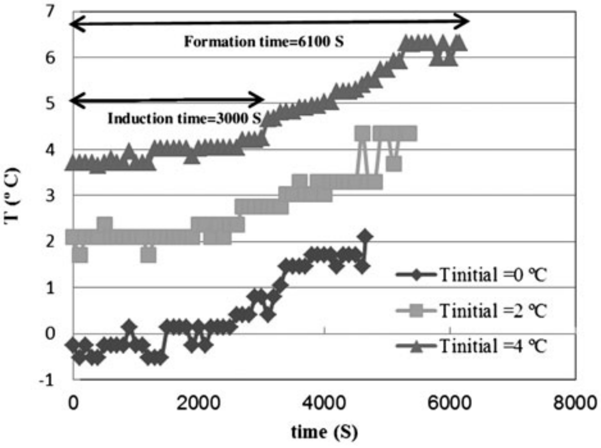

Fig. 4. Temperature–time profile during R141b hydrate formation at different initial temperatures for saline solution of NaCl 4%.

effect of temperature was clearly shown on the formation rate. The rate of formation decreases at higher initial temperatures due to decreased driving force.

Results presented in Figs. 2–4 indicate that the kinetic behavior of R141b hydrate formation is dependent on saline concentration and initial temperature. Generally the lower temperatures produce more rates of hydrate formation. Also, the higher saline concentrations decrease the formation rate at a given temperature and increase the induction time. Induction time is a part of the process where conditions are suitable for the appearance of initial nuclei in the reactor. The results are given in Table 1 for different experimental conditions. For example, the induction and formation time were identified at temperature 4°C for 0 and 4% saline solution in Figs. 3 and 4.

The data were obtained by measuring the temperatures of hydrate–liquid–liquid solution in the reactor during the growth time of hydrate. As shown in Fig. 3, it seems that the linear relation of the temperature–time profiles can be used to evaluate the hydrate formation rate according to the analysis given below.

Hydrate formation is an exothermic process, so the heat of hydrate formation is introduced in the system as sensible heat that increases the temperature of the solution [19]. Since the system was assumed adiabatic, the relationship between hydrate growth and the temperature of solution was given by Eq. (2) [19].

$$R \times \Delta H = \{T/t\} \times \{m_{\mathrm{w}}Cp_{\mathrm{w}} + m_{\mathrm{g}}Cp_{\mathrm{g}}\} \tag{2}$$

In Eq. (2), the quantities are defined:

R: rate of hydrate formation (mol/s); ΔH: heat of hydrate formation (J/mol); T/t: rate of temperature increase during hydrate growth (°C/s); m_{w}, m_{g}: mass of water (or saline solution) and guest species (R141b); Cp_{W}, Cp_{g}: specific heat capacity of water and guest species (R141b).

The mass and specific heat capacity of water and R141b are given in Table 2.

The rate of R141b hydrate formation was calculated using Eq. (2) and data presented in Figs. 2–4. Then, the obtained results were plotted in Fig. 5 at three different initial temperatures: 0, 2, and 4°C. Fig. 5 indicates the dependence of incorporation rate of water into hydrate on temperature and saline concentration. According to Fig. 5, a linear relation can be considered between the formation rate and initial temperatures. The correlation coefficient (R^2) of obtained curves nears 1 for both 0 and 4% saline solutions.

Table 1
Induction and formation time of R141b hydration process at different temperatures for NaCl saline solution

Concentration of NaCl (% wt)	$T_{\text{initial}} = 0^\circ\text{C}$		$T_{\text{initial}} = 2^\circ\text{C}$		$T_{\text{initial}} = 4^\circ\text{C}$	
	Induction time (s)	Formation time (s)	Induction time (s)	Formation time (s)	Induction time (s)	Formation time (s)
0	480	2040	1,200	3,480	2040	3,840
1	900	3,300	–	–	–	–
2	1,200	4,500	–	–	–	–
4	2,100	4,800	2,400	5,400	3,000	6,100
6	2,700	5,100	–	–	–	–

Table 2
Values of mass and specific heat capacity

Component	*M* (kg)	*Cp* (J/kg°C)
H_2O	0.225	4,187
R141b	0.0915	1,160

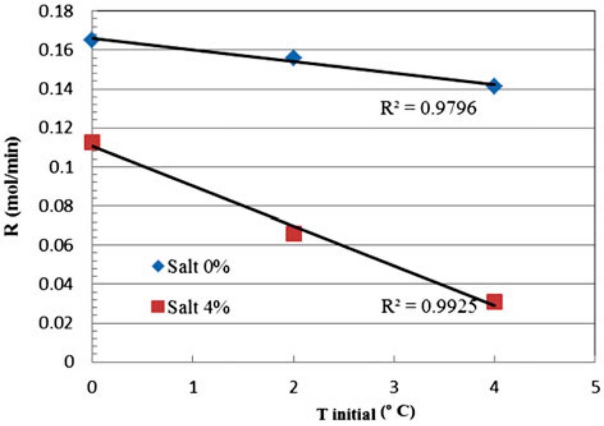

Fig. 5. Rate of R141b hydrate formation for saline solution of NaCl.

3.2. Effects of salt on process

Salts are effective on hydrate formation by increasing the equilibrium pressure at certain temperature or decreasing the equilibrium temperature at certain pressure [19]. The degree of super-cooling is simply calculated as $(T - T_{\text{eq}})$ where T_{eq} depends on the concentration and type of salt in solution [19]. Fig. 2 shows that the equilibrium temperature is decreased from 2.5°C in pure water to 1.4°C in 6 wt% NaCl.

Salts have an inhibiting effect on hydrate formation, so the rate of nucleation and growth reduces in presence of salts due to the reduction of cavity in surface [21]. Based on the investigation of researchers, the inhibition effect of salts in the hydrate process strongly depends on the ionic size and electrical charge [3]. The inhibiting strength has the straight relation with the number of electrical charges and the inverse relation with ionic size [3].

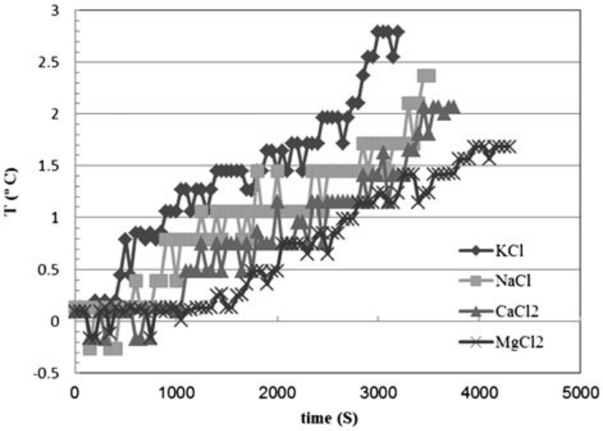

Fig. 6. Temperature–time profile during R141b hydrate formation at initial temperature of 0°C for different solutions of salts (0.304 mol/L).

In brine sea water, salts of KCl, $MgCl_2$, and $CaCl_2$ exist along NaCl salt. Therefore, a number of experiments were performed by using solutions with the similar molarity 0.304 mol/L of named salts to investigate the effect of these salts on the growth process of R141b hydrate. Fig. 6 shows the temperature–time profile of R141b hydrate experiment at initial temperature of 0°C for different solutions of the above mentioned salts. As seen in Fig. 6, by comparing the kinetic curves and equilibrium temperatures, it can be seen that the order of inhibition strength among metal chlorides is: $Mg^{+2} > Ca^{+2} > Na^{+1} > K^{+1}$. The separation of crystals from brine water was accomplished by compressing process (described in part 2.3).

3.3. Desalination of brine solution by R141b hydrate

A hydrate freezing process can be considered very similar to a freezing process for desalination. In this process, hydrate former (gas or liquid) and water must be mixed and then hydrates will be precipitated [3–5,22]. The crystals are physically separated from the remaining brine, washed, and then melted. An advantage of the process is the fact that it can operate at a higher temperature than a freezing process. Therefore, the energy requirements of the process decrease [3,23].

Almost the hydrate crystals of R141b were observed on the surface of saline solution. After the completion of process, as described in part (2–3), the squeezing operation was used for separating crystals. Fig. 7 shows the hydrate pellets of R141b after squeezing stage. Subsequently, the electrical conductivity of residual distilled water was measured after heating crystals and voiding R141b steams. Then the removal efficiency of salt was determined during hydrate process by Eq. (3).

$$\text{Efficiency }(\%) = \frac{\text{Initial conductivity} - \text{Final conductivity}}{\text{Initial conductivity}} \times 100 \tag{3}$$

The efficiency of desalination process was presented for different concentrations of salt and different temperatures in Tables 3 and 4, respectively. The results show that the removal efficiency by hydrate method increases at the higher concentrations of salt in initial solution and lower temperatures.

Table 4
The desalination efficiency for NaCl saline solution of 4%

T_{initial} (°C)	0	2	4
Initial conductivity at 15°C (mS/cm)	75.00	75.00	75.00
Final conductivity at 15°C (mS/cm)	28.90	35.50	38.30
Efficiency (%)	61.49	52.66	48.93

Table 5
The desalination efficiency at $T_{\text{initial}} = 0$°C and molarity 0.304 mol/L of different salts

Salt type	NaCl	KCl	$MgCl_2$	$CaCl_2$
Initial conductivity at 15°C (mS/cm)	35.50	43.15	27.83	67.46
Final conductivity at 15°C (mS/cm)	11.68	12.79	11.41	26.30
Efficiency (%)	67.09	70.73	59.00	61.01

The desalination efficiency with different salts is given in Table 5. The removal efficiency for ions of groups I and II is in the order: $K^{1+} > Na^{1+} > Ca^{2+} > Mg^{2+}$. Thus, the removal of alkaline metals is better than that of alkaline earth metals by the hydrate-based desalination process. However, the removal efficiency depends on the ionic size and the number of electrical charge. Generally salts with higher ionic sizes and lower charge numbers improve the desalination efficiency. The results presented by Park et al. based on water desalination by CO_2 hydrate formation [3] confirm the results given in this paper.

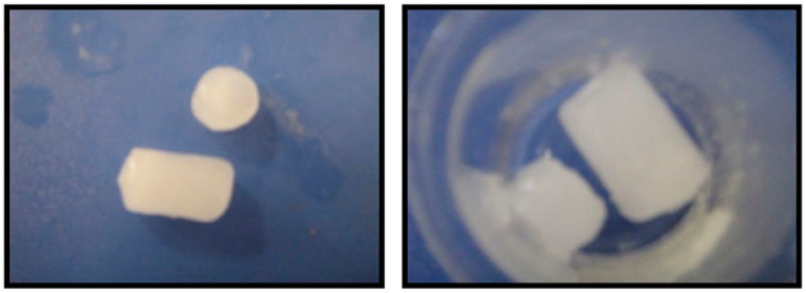

Fig. 7. Hydrate crystal of R141b.

Table 3
The desalination efficiency at $T_{\text{initial}} = 0$°C

Salt concentration (% wt)	0	1	2	4	6
Initial conductivity at 15°C (mS/cm)	2.64×10^{-3}	17.30	40.00	75.00	98.30
Final conductivity at 15°C (mS/cm)	1.35×10^{-3}	8.50	14.50	28.90	34.30
Efficiency (%)	48.86	50.86	63.75	61.46	65.10

5. Conclusion

In this paper, to study the kinetic behavior associated R141b hydrate growth, the experiments were performed in a cylindrical glass reactor at initial temperatures of 0, 2, and 4℃ for saline concentrations of 1, 2, 4, and 6% weight of NaCl and also, the molarity 0.304 mol/L of NaCl, KCl, $CaCl_2$ and $MgCl_2$ aqueous solutions. The feasibility of desalination by R141b hydrate formation was also investigated in different brine solutions. We conclude the following based on our experimental data in this study:

(1) The rate of R141b hydrate formation is dependent on the saline concentration, initial temperature, and type of salt. Generally, the lower temperatures and lower saline concentrations provide faster rates of hydrate formation and decrease the induction time.

(2) The inhibition effect of salts depends on the ionic size and electrical charge strongly in hydrate formation process. The inhibition strength for metal chlorides is: $Mg^{2+}>Ca^{2+}>Na^{1+}>K^{1+}$.

(3) The results of desalination process show that the removal efficiency is further at the lower temperatures and higher concentrations of salt. Also, the removal of alkaline metals is better than that of alkaline earth metals by hydrate-based desalination process. The maximum and minimum removal percents are 70 and 59% for KCl and $MgCl_2$ salts, respectively.

References

[1] E.D. Sloan, Clathrate Hydrates of Natural Gases, Marcel and Dekker, New York, 1998.

[2] A.L. Ballard, E.D. Sloan, Hydrate phase diagrams for Methane+ Ethane+ Propane mixtures, Chem. Eng. Sci. 56(24) (2001) 6883–6895.

[3] K.N. Park, S.Y. Hong, J.W. Lee, K.C. Kang, Y.C. Lee, M.G. Ha, J.D. Lee, A new apparatus for seawater desalination by gas hydrate process and removal characteristics of dissolved minerals (Na^+, Mg^{2+}, Ca^{2+}, K^+, B^{3+}), Desalination 274 (2011) 91–96.

[4] P.M. Williams, M. Ahmad, B.S. Connolly, Freeze desalination: An assessment of an ice maker machine for desalting brines, Desalination 308 (2013) 219–224.

[5] Y. Mandri, A. Rich, D. Mangin, S. Abderafi, C. Bebon, N. Semlali, J.P. Klein, Parametric study of the sweating step in the seawater desalination process by indirect freezing, Desalination 269 (2011) 142–147.

[6] A. Rich, Y. Mandri, D. Mangin, A. Rivoire, Sea water desalination by dynamic layer melt crystallization: Parametric study of the freezing and sweating steps, J. Crys. Growth. 342 (2012) 110–116.

[7] A.M. Aliev, R.Y. Yusifov, A.R. Kuliev, Y.G. Yusifov, Method of gas hydrate formation for evaluation of water desalination, Russ. J. Appl. Chem. 81 (2008) 588–591.

[8] D. Corak, T. Barth, T. Skodvin, R. Larsen, T. Skjetne, Effect of subcooling and amount of hydrate former on formation of cyclopentane hydrates in brine, Desalination 278 (2011) 268–274.

[9] A. Parker, Potable water from sea water, Nature 149 (1942) 184–186.

[10] Y.T. Ngan, P. Englezos, Concentration of mechanical pulp mill effluents and NaCl Solutions through propane hydrate formation, Ind. Eng. Chem. Res. 35 (1996) 1894–1900.

[11] K.H. Guo, B.F. Shu, Y. Zhang, Transient behavior of energy charge-discharge and solid-liquid phase in change mixed gas hydrate formation, in: BX. Wang (Ed.), Heat Transfer Science and Technology, Higher Education Press, Beijing, 1996, pp. 728–733.

[12] Y. Bi, T. Guo, T. Zhu, S. Fan, D. Liang, L. Zhang, Influence of volumetric flow rate in the crystallizer on the gas hydrate cool storage process in a new gas hydrate cool storage system, Appl. Energy 78 (2004) 111–121.

[13] J. Li, K. Guo, D. Liang, R. Wang, Experiments on fast nucleation and growth of HCFC141b gas hydrate in static water columns, Int. J. Refrig. 27 (2004) 932–939.

[14] F. Isobe, Y.H. Mori, Formation of hydrate or ice by direct-contact evaporation of cfc alternatives, Int. J. Refrig. 15(3) (1992) 137–142.

[15] K. Maeda, Y. Katsura, Y. Asakuma, K. Fukui, Concentration sodium chloride in aqueous solution by chlorodifluoromethane gas hydrate, Chem. Eng. Process 47 (2008) 2281–2286.

[16] P. Englezos, P.R. Bishnoi, Prediction of gas hydrate formation conditions in aqueous electrolyte solutions, A.I.Ch.E.J 34(10) (1988) 1718–1721.

[17] H. Kubota, K. Shimizu, Y. Tanaka, T. Makita, Thermodynamic properties of R13 (CClF3), R23 (CHF3), R152a (C2H4F2), and propane hydrates for desalination of sea water, J. Chem. Eng. Jpn. 17(4) (1984) 423–429.

[18] A.J. Barduhn, H.E. Towlson, Y.C. Hu, The properties of some new gas hydrates and their use in demineralizing sea water, A.I.Ch.E.J. 8(2) (1962) 176–183.

[19] R.W. Bradshaw, D.E. Dedrick, B.A. Simmons, J.A. Greathouse, R.T. Cygan, E.H. Majzoub, Desalination Utilizing Clathrate Hydrates, Sandia National Laboratories, California, 2008.

[20] Y. Xie, K. Guo, D. Liang, Sh. Fan, J. Gu, Steady gas hydrate growth along vertical heat transfer tube without stirring, Chem. Eng. Sci. 60 (2005) 777–786.

[21] J.P. Lederhos, J.P. Long, R.L. Christiansen, E.D. Sloan, Effective kinetic inhibitors for natural gas hydrates, Chem. Eng. Sci. 51 (1996) 1221–1229.

[22] T. Younos, K.E. Tulou, Overview of desalination techniques, J. Cont. Water Res. Educ. 132 (2005) 3–10.

[23] J.D. Lee, Y.S. Kim, H.J. Lee, Y.D. Kim, A study of desalination using CO_2 hydrate technology, The 6th Int. Conference on Gas Hydrates, Vancouver, BC, Canada, July 6–10, 2008.